Supplementary material of

Estimating Greenland ice sheet surface mass balance contribution to future sea level rise using the regional atmospheric climate model MAR

Fettweis et al., TC, 2013

Table of Contents

1 Comparison of MARv1, MARv2 and RACMO2 over current climate

According to Section 2.1, MAR was run over two different ice sheet masks and the smoothing of the ice sheet topography (needed for the stability of MAR) is reduced by a factor 2 in the CMIP5 forced MAR simulations (called MAR version 2) in respect to the MAR future projections made for ICE2SEA using HadCM3 and ECHAM5 as forcing (called MAR version 1).

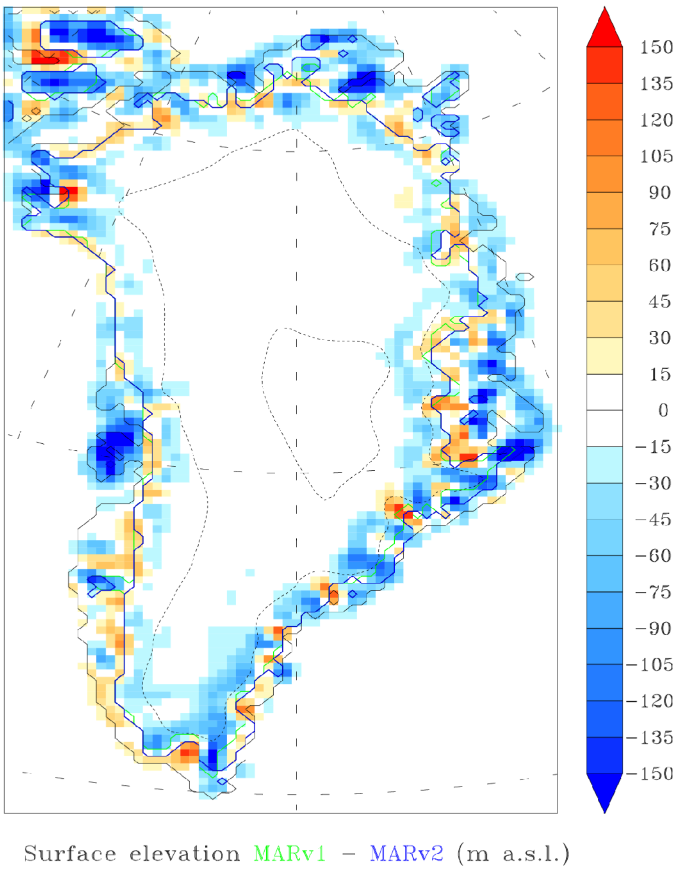

***Fig. S1**: Surface elevation differences between MARv1 and MARv2. The ice sheet mask used in the two different simulations is also plotted in blue (MARv2) and in green (MARv1).*

Due to the extension of the ice sheet mask in MARv2, the SMB components integrated over the whole ice sheet are generally 6% larger in MARv2 than in MARv1 (see Table S1), but the related interannual variability compares very well between ERA-40 forced MARv1 and MARv2 (see Fig. S3), with correlation coefficients higher than 0.99 for the period 1980--1999 (see Table S2). In 2D, the differences are not significant (see Fig. S2) in respect to the differences shown by Fig. 1 using the different forcings.

That is why, the ERA-40/ERA-INTERIM forced MAR simulations using the different ice sheet topographies/masks over 1960-2010 was used to cross-calibrate the results when values of SMB components are given at the scale of the whole ice sheet. However, the MARv1 based future projections are only given here by way of comparison but not used in our estimations of future SLR.

	SMB	Snowfall	Run-off
MAR version 1	248±41	649±67	281±97
MAR version 2	232±39	614±65	272±97

Table S1*: Average and standard deviation of SMB using both setups forced by the ECMWF reanalyses over 1960-2010. Units are GT/yr.*

	SMB		Snowfall		Run-off	
	corr.	rmse	corr.	rmse	corr.	rmse
MARv1 vs MARv2 ERA-40 (1980-1999) – ERA-INTERM (2000-2010)	1.00	25	0.98	36	1.00	16
RACMO2 vs MARv2 ERA-40 (1980-1988) – ERA-INTERM (1989-2011)	0.94	49	0.92	51	0.95	32
MARv2 (ERA-40) vs MARv2 (ERA-INTERIM) 1980-1999	0.98	62	0.95	39	0.98	23

Table S2*: Statistics (coefficient of correlation and RMSE in GT/yr) comparing time series plotted in Fig. S1. The ECMWF reanalyses used as forcing and the period over which the statistics are computed are listed in the table. It should be noted that the comparison between MAR and RACMO is made here on the ice sheet mask own to each model and that RACMO2 was run at a resolution of 11 km.*

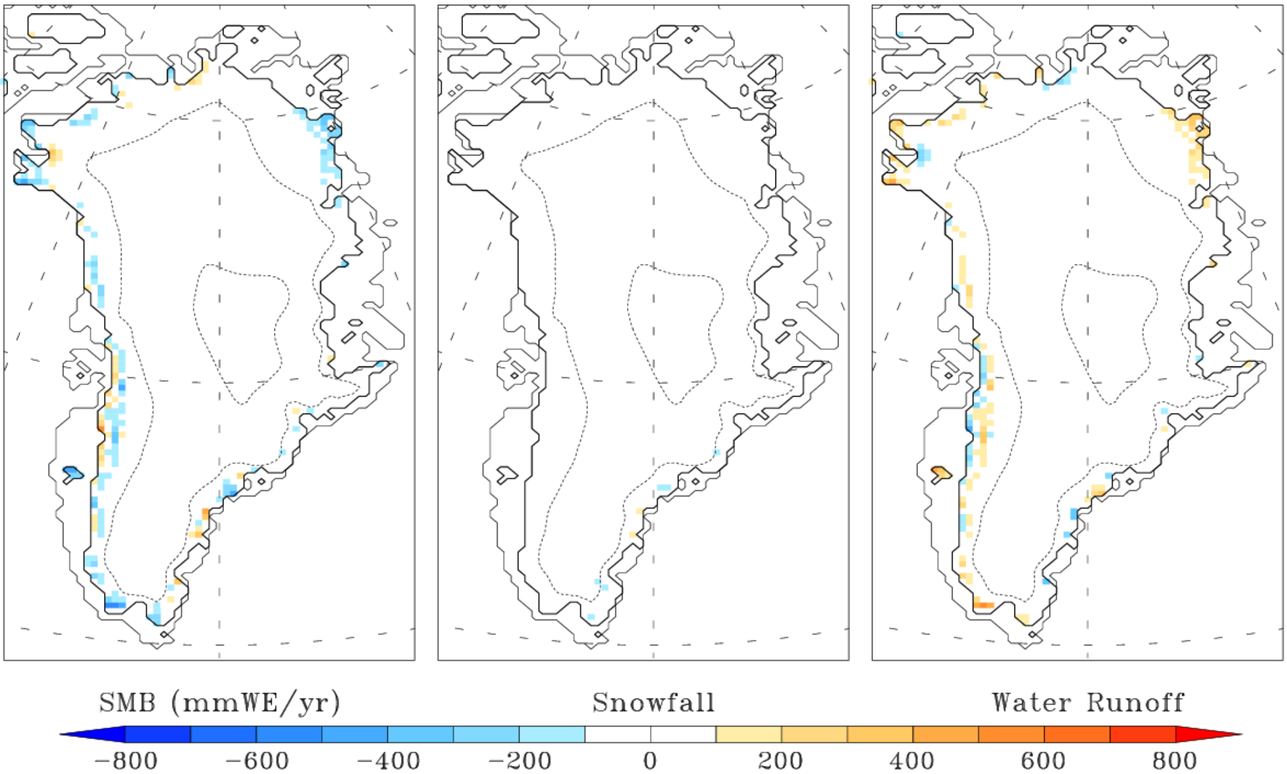

***Fig. S2**: The mean difference of the annual SMB, snowfall and water run-off between MARv1$_{ERA\text{-}40}$ and MARv2$_{ERA\text{-}40}$ over 1980-1999. This figure is similar to Fig. 1 in the manuscript.*

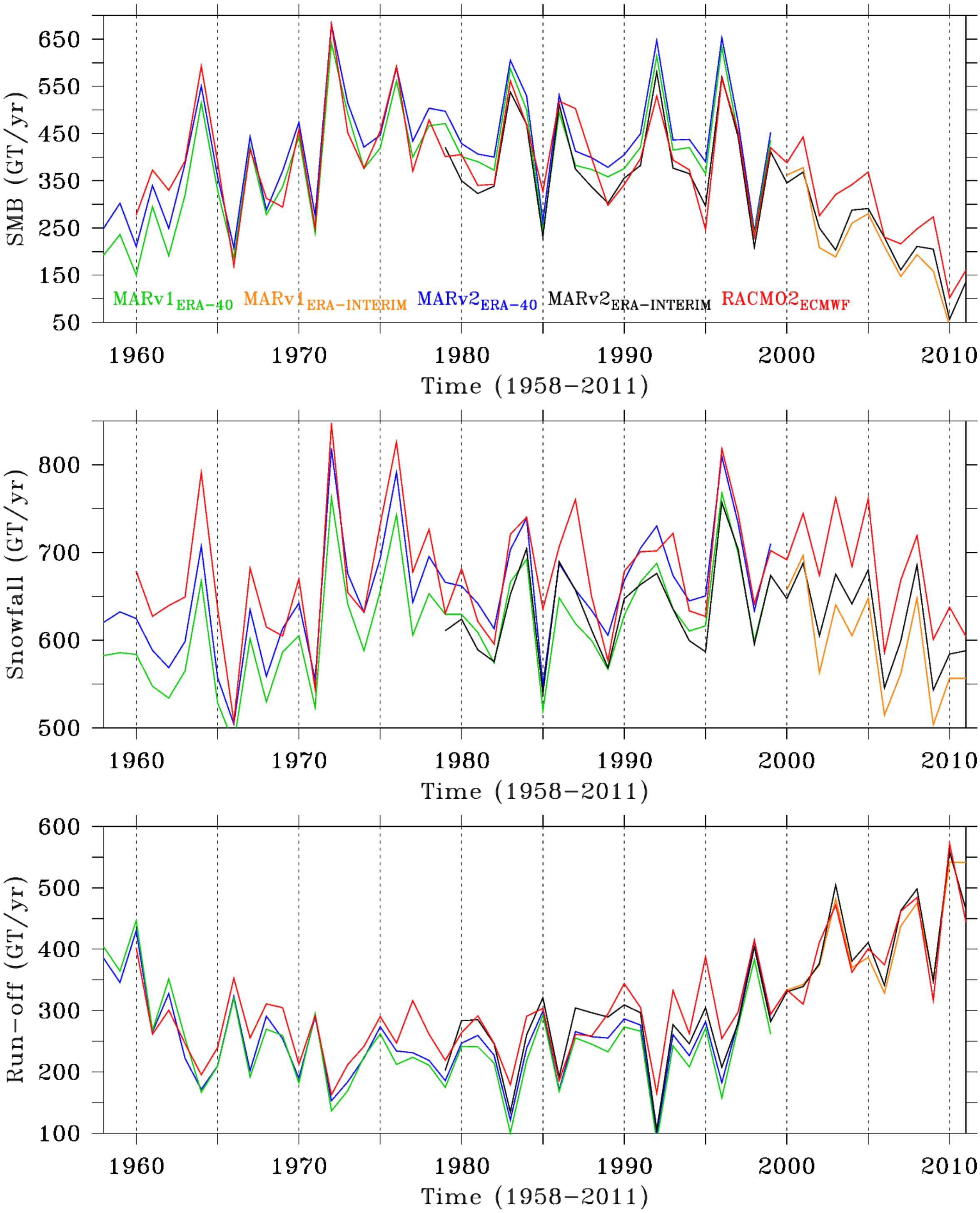

***Fig. S3**: Time series of the annual total ice sheet SMB, snowfall and run-off (in GT/yr) simulated by MAR and RACMO2 forced by the ECMWF reanalyses. RACMO2 is forced by ERA-40 over 1960-1988 and by ERA-INTERIM over 1989-2011.*

2 Evaluation of the CMIP5 forced MAR simulations over 1970-1999

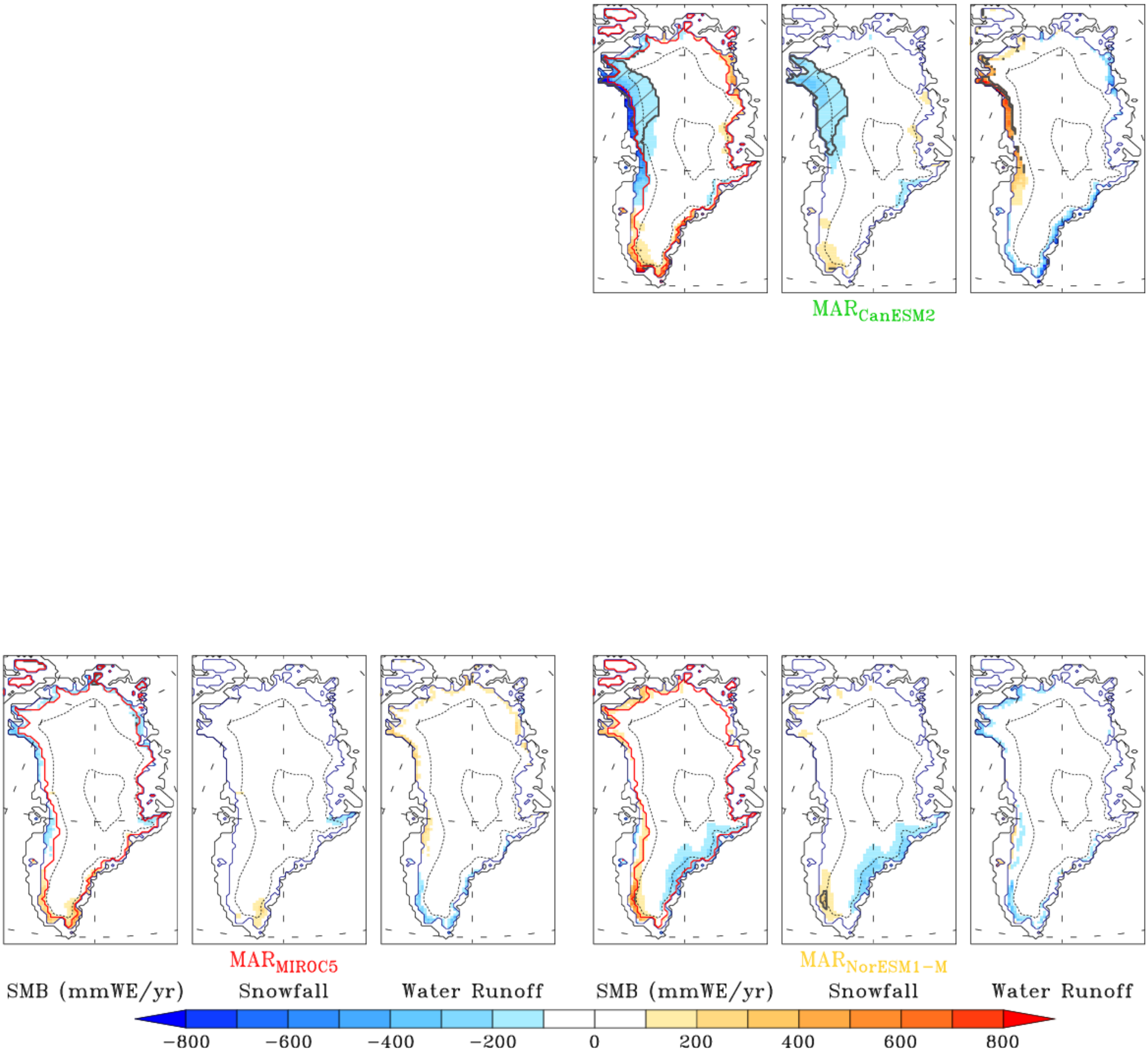

Fig. S4: *Mean anomalies of the annual SMB, snowfall and water run-off with respect to the ERA-40-forced MAR simulation over 1970--1999 for the MAR simulations listed in Table 2. . Units are mmWE/yr. The areas where the anomalies are two times above the 1970-1999 standard deviation of MAR_{ERA-40} are hatched in dark grey. The ELA from MAR_{ERA-40} is plotted in red. This figure is similar to Fig. 1 in the manuscript.*

3 Evaluation of 30 CMIP5 GCMs over current climate (1980-1999)

Lists of the CMIP5 GCMs for which biases in the current summer T700 are acceptable i.e. without significant biases (see Fig. S5a):
BNU-ESM, **CanESM2**, CMCC-CM, CNRM-CM5, CSIRO-MK3, FIO-ESM, IPSL-CM5A-MR, **MIROC5**, MPI-EMS-LR, MPI-EMS-MR, **NORESM1-M**

Lists of the CMIP5 GCMs for which biases in the current Z500 pattern (described in the text) are acceptable at the MAR boundaries (see Fig. S5b):
ACCESS1, **CanESM2**, BNU-ESM, CCSM4, CESM1-BGC, CMCC-CM, CNRM-CM5, FGOAL-s2, GFDL, HadGEM2-CC, HadGEM2-ES, IPSL-CM5A-MR, **MIROC5**, MPI-ESM, **NorESM1-M**

Lists of the previous CMIP5 GCMs for which biases in the current wind speed at 500 hPa at the MAR boundaries are acceptable:
ACCESS1, **CanESM2**, CCSM4, CMCC-CM, FGOAL-s2 , GFDL, HadGEM2-CC, HadGEM2-ES, **MIROC5**, **NorESM1-M**

Lists of the CMIP5 GCMs selected by *Belleflamme et al. (2012)*:
in summer (JJA): BCC, BNU-ESM, **CanESM2**, **MIROC5**, MPI-ESM-MR and **NorESM1-M**
in winter (DJF): BNU-ESM, HadGEM2-ES, MPI-ESM-LR, MPI-ESM-MR and **NorESM1-M**

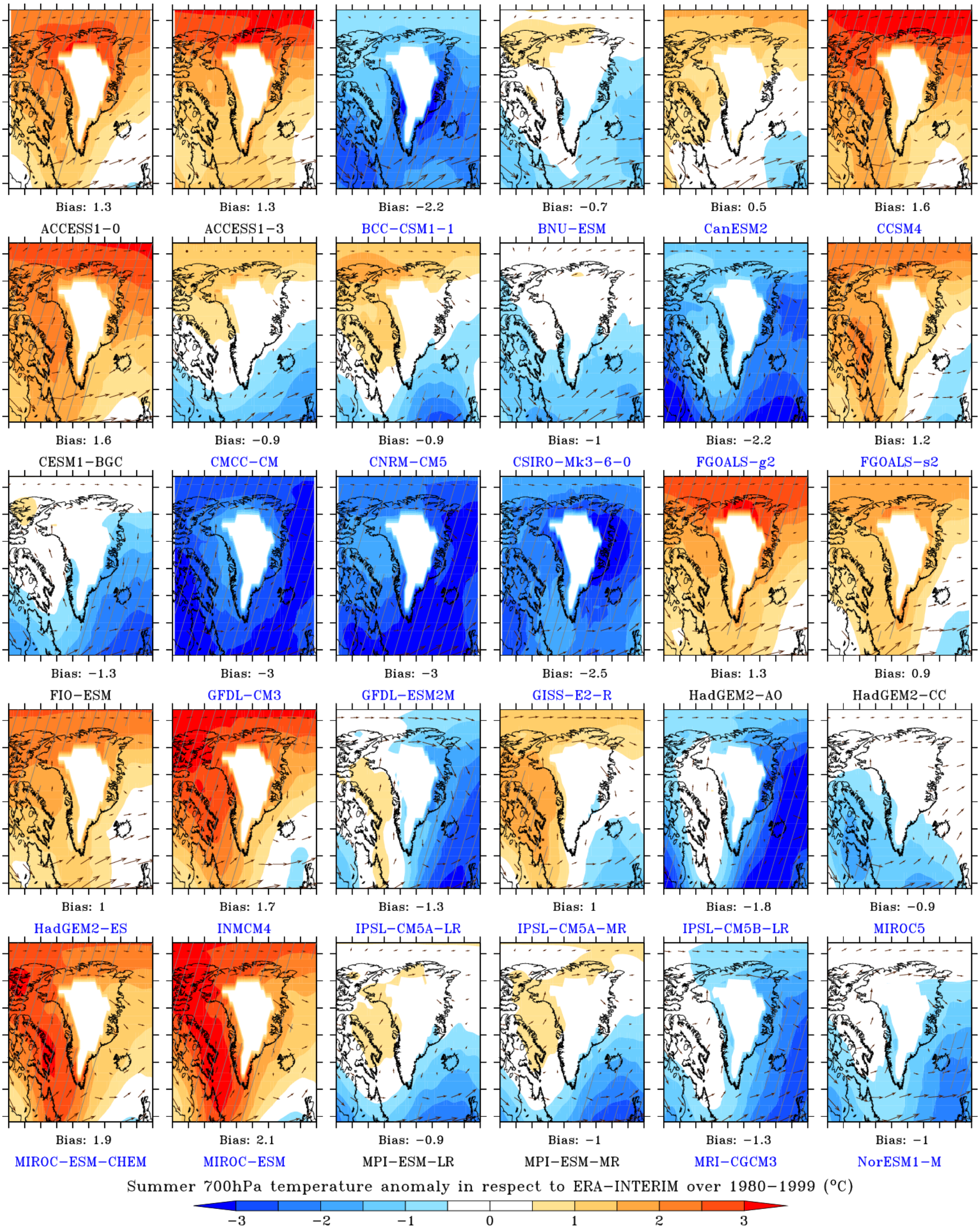

Fig. S5a: *Mean anomalies of the JJA 700hPa Temperature simulated by the 30 CMIP5 GCMs used in the CMIP5 ensemble mean with respect to ERA-INTERIM over 1980--1999. The JJA mean wind vectors (not anomalies) at 700hPa are also plotted and the mean temperature bias is listed in normalised value. The areas where the anomalies are* *two times above the 1980-1999 standard deviation of ERA-INTERIM are hatched in dark grey. Finally, the GCMs for which 6 hourly outputs are available in the CMIP5 database are listed in blue. This figure is similar to Fig. 2 in the manuscript.*

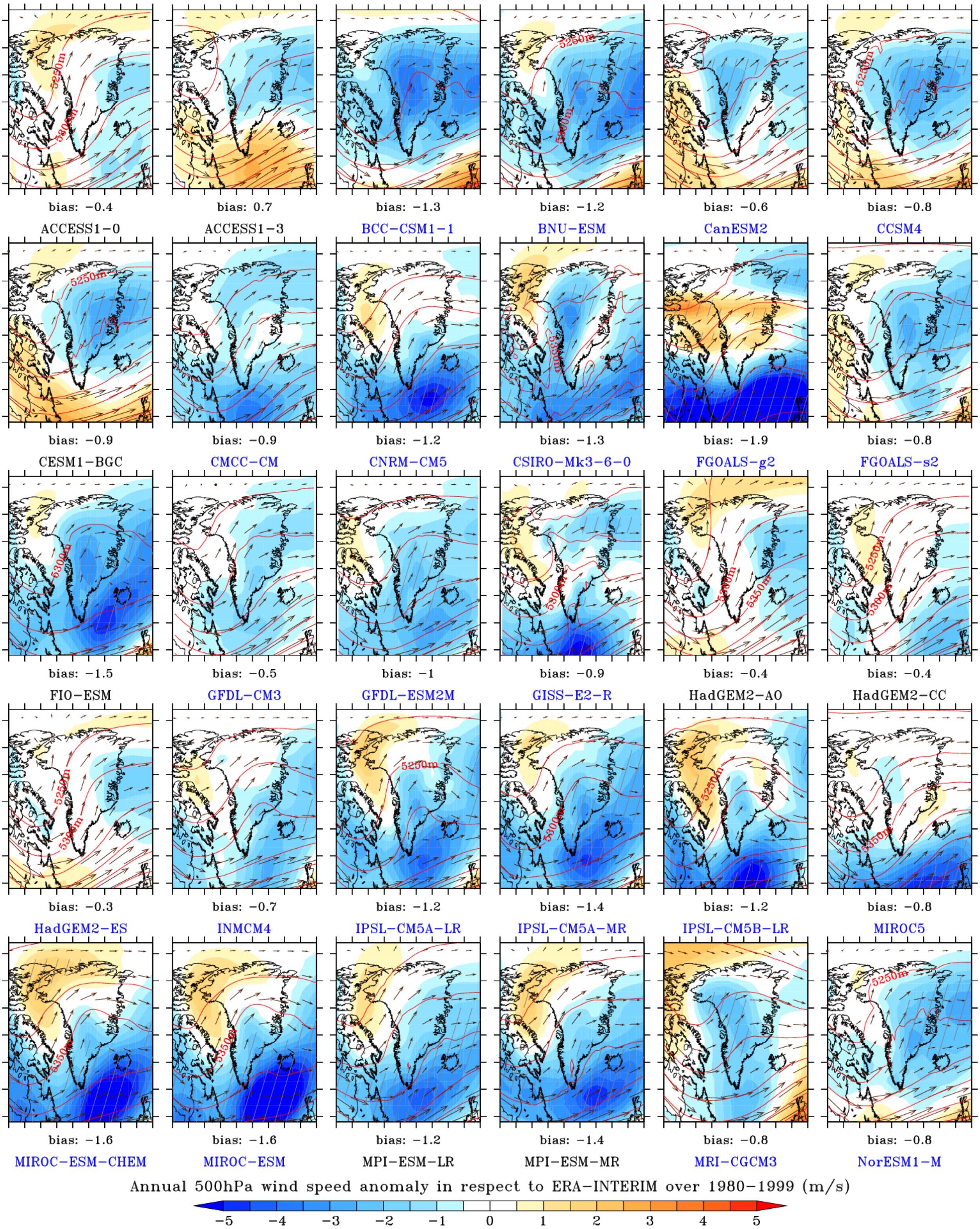

Fig. S5b: *Same as Fig S5a but the annual mean wind speed at 500hPa. The annual mean Z500 and wind vectors at 500hPa are also plotted. Finally, it should be noted that a similar comparison limited to the summer (JJA) is available in Belleflamme et al. (2012) in respect to the NCEP-NCAR reanalysis over 1960-1990.*

4 Evaluation of the chosen CMIP5 GCMs over 1960-2010

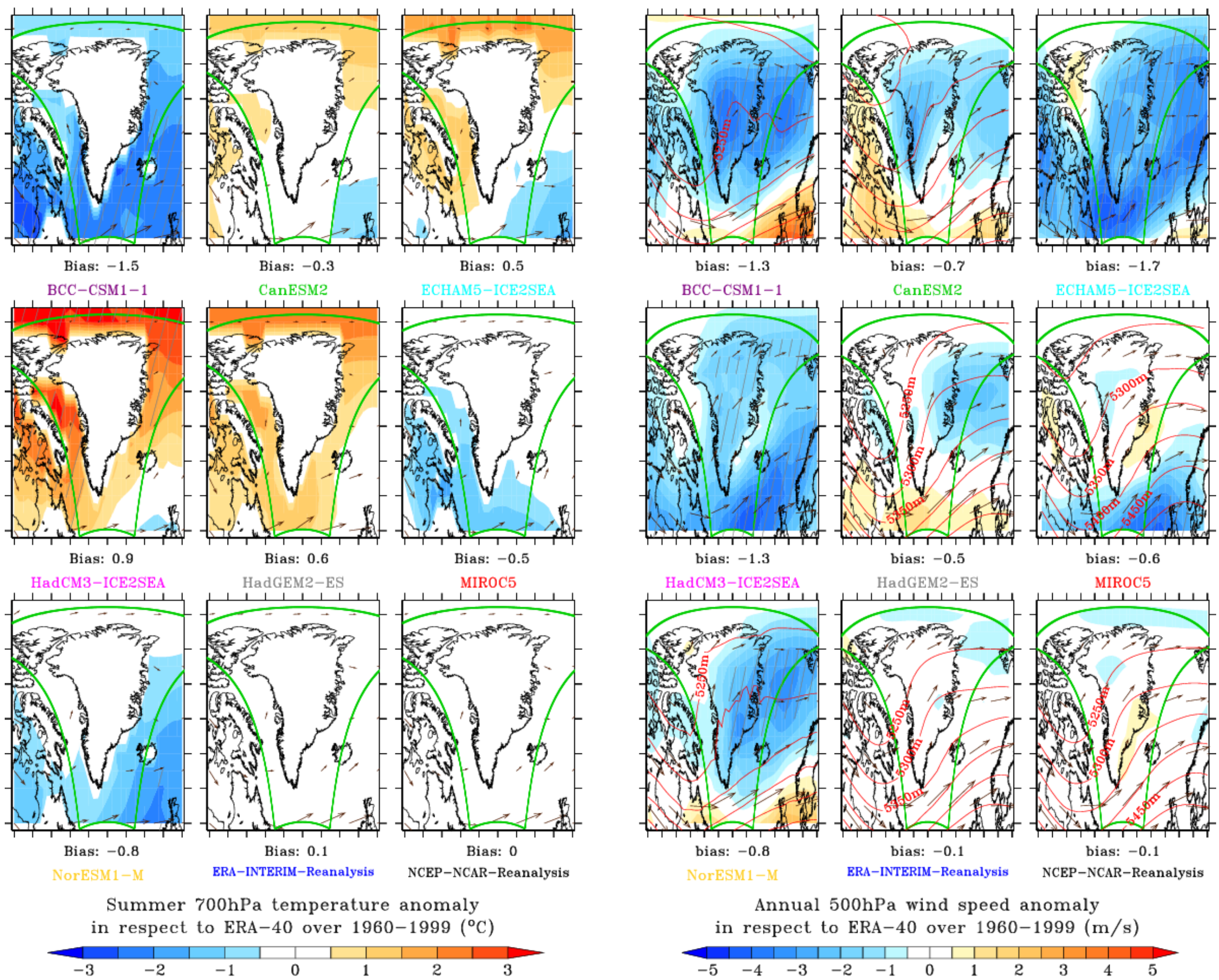

Fig. S6 *Mean anomalies of the JJA 700hPa Temperature simulated by the different GCMs used in this study with respect to ERA-40 over 1970-1999. The JJA mean wind vectors (not anomalies) at 700 hPa are also plotted and the mean temperature bias is listed in normalised value. Finally, the boundaries of the MAR integration domain are plotted in green and the areas where the anomalies are two times above the 1970--1999 standard deviation of ERA-40 are hatched in dark grey. (Right) Same as (left) but for the annual mean wind speed at 500 hPa. The annual mean wind vectors at 500 hPa and isohypses of the geopotential height at 500 hPa are also plotted in black and red respectively. This figure is similar to Fig. 2 in the manuscript.*

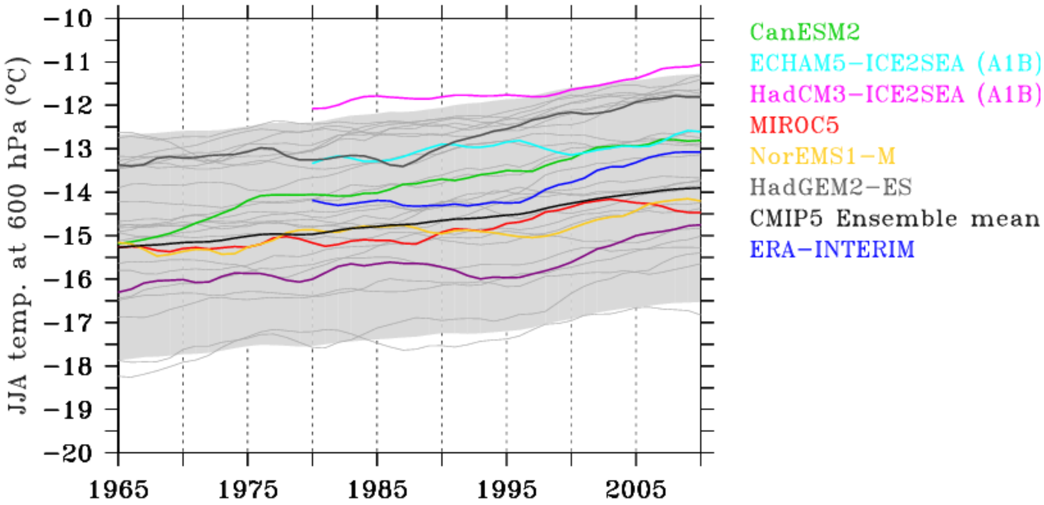

Fig. S7. *Time series over 1965-2010 of the JJA T600 over Greenland in absolute value (not in anomaly here). A 10-yr running mean is applied here.*

This figure shows well that the decadal variability in the time series does not explain the biases in the CMIP5 GCM and that changing of reference period does not change here the conclusion of our evaluation. For example, HadGEM2-ES (resp. BCC-CSM1) is too warm (resp. too cold) over the whole period presented here.

5 Evaluation of the current seasonal variability over 1980-1999

The simulations that best simulate the seasonality (i.e. an amplitude of ~25°C between summer and winter) of the near-surface temperature (TAS) are MAR_{ECHAM5}, MAR_{MIROC5} and $MAR_{NorESM1\text{-}M}$ with respect to $MAR_{ERA\text{-}INTERIM}$ (see Fig. S8a). The $MAR_{CanESM2}$ simulation is too cold in winter while MAR_{HadCM3} is too warm in summer and $MAR_{BCC\text{-}CSM1\text{-}1}$ is too cold through the whole year. Finally, it should be noted that $MAR_{ERA\text{-}40}$ is 0.25-0.5°C too cold every month with respect to $MAR_{ERA\text{-}INTERIM}$, which gives an idea of the uncertainties in the reanalyses-forced MAR simulations.

On average, the MAR simulations that are too warm (resp. cold) in summer overestimate (resp. underestimate) the run-off (see Fig. S8c). However, MAR_{ECHAM5} overestimates the run-off while the TAS anomalies are lower than +0.5°C in summer. This is due to a relatively longer exposure of bare ice areas in summer resulting from the underestimation of snowfall.

The MAR_{MIROC5} best simulates the seasonality of snowfall with a maximum in fall and a minimum in summer (only the anomalies are shown in Fig. S8e). The underestimation of snowfall by $MAR_{BCC\text{-}CSM1\text{-}1}$ results from the underestimation of the general circulation dynamic by BCC-CSM1-1 and from the too low temperatures in winter, that prevents heavy precipitation events.

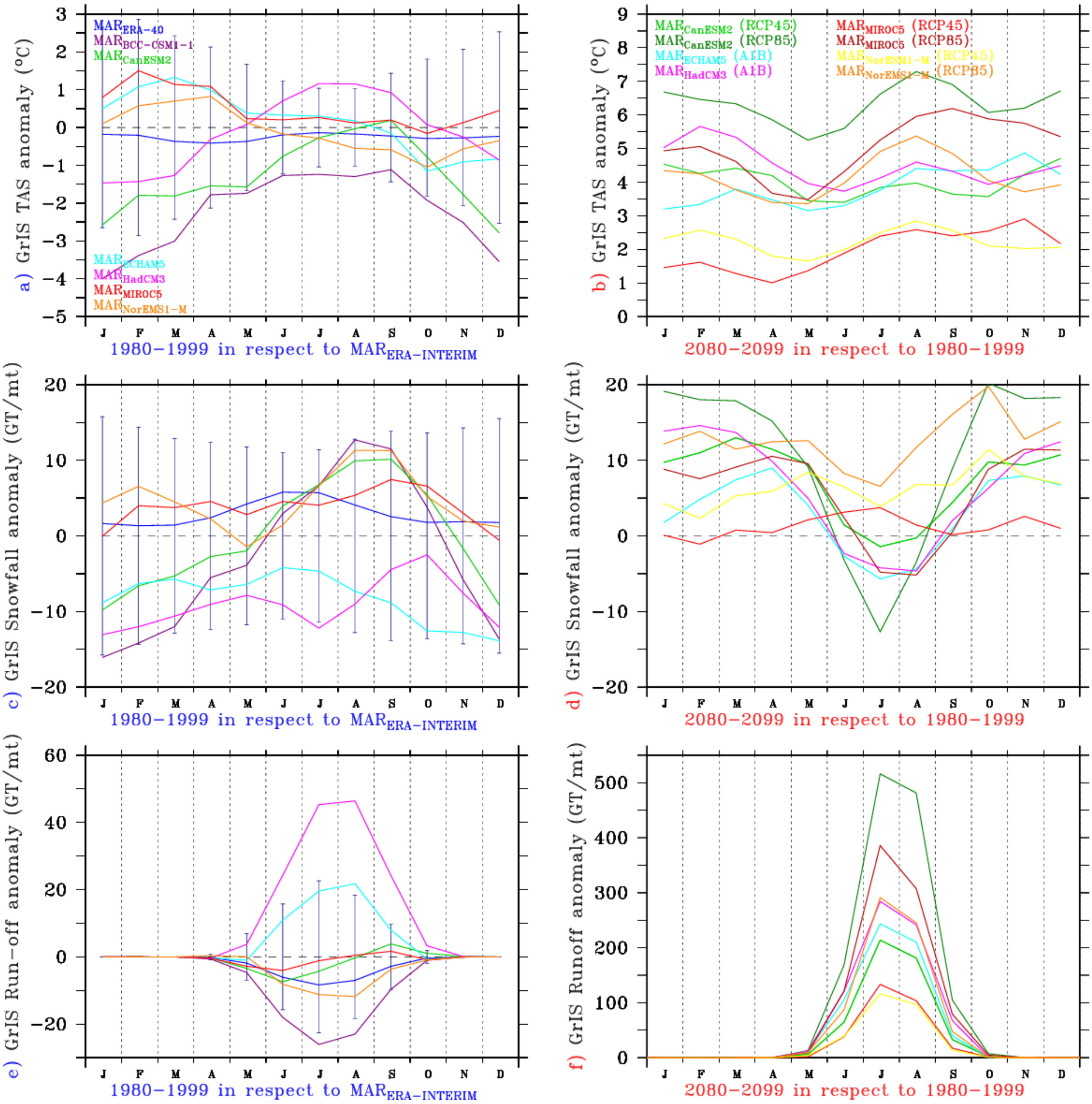

Fig. S8 *a) Monthly anomalies of the GrIS TAS (in°C) simulated by MAR forced by the different listed GCMs with respect to MAR$_{ERA\text{-}INTERIM}$ over 1980-1999. The error bars show the standard deviation of the MAR$_{ERA\text{-}INTERIM}$ simulation over 1980-1999. b) Same as a) but for the GrIS TAS anomalies over 2080-2099 with respect to MAR forced by the same GCM over 1980-1999. c) Same as a) but for the GrIS monthly cumulated snowfall in GT/month. d) Same as b) but for the snowfall. e) Same as a) but for the GrIS monthly cumulated water run-off in GT/month. f) Same as b) but for the water run-off. Finally, a 3-month running mean is applied on each time series for smoothing the curves except in Fig. S8f.*

6 Evaluation of the future seasonal variability over 2080-2099

The increase of temperature is not projected to occur uniformly through the year as shown in Fig. S8b. A first peak should occur in summer (August), likely due to the amplification of the albedo feedback mechanism because this peak is higher for the simulations with the greatest change in ELA. A second peak is projected to occur in winter (January) when the impact of the sea ice decline is the highest over Greenland according to Deser et al. (2010)[1].

However, in these scenarios we see little seasonal change in the components of the SMB. The melting season should still be limited to the current melting season (from May to September), even for extreme CO2 scenarios, as the one obtained in the case of $MAR_{CanESM2}$ as shown by Franco et al. (2012b). The highest water run-off increase will occur in July and August but no considerable run-off increase is projected in May. Finally, it should be noted that no change in the daily TAS variability is projected knowing that temperature daily variability becoming greater should impact the amount of melt as the extreme event observed on Mid-July 2012 (Nghiem et al., 2012)[2].

Due to rising temperature, most of the simulations indicate a decrease in snowfall to the benefit of rainfall, which enhances the melt. These changes are particularly evident in the ablation zone, where most of the precipitation is projected to occur in liquid phase during summer at the end of this century. An increase in summer snowfall in the percolation zone would result in a negative albedo feedback (Box et al., 2012.), but no such snowfall change occurs in the MAR simulations. In the current dry snow zone, more frequent fresh snow events will increase surface albedo during summer but this negative albedo feedback is dampened by the increasing melt for warming exceeding 4°C, as explained by Franco et al. (2012).

Snowfall is only projected to increase during the winter season, delaying the appearance of multi-year snow or bare ice (with a lower albedo) once the winter snowpack is completely removed by melting. This explains why no water run-off increase is projected in May with respect to the current climate while higher TAS are projected in May.

Finally, it should be noted that the projected snowfall changes are in the same range of the snowfall biases over current climate with respect to $MAR_{ERA\text{-}INTERIM}$ (Figs. S8c, d) while the run-off biases over 1980--1999 are negligible with respect to the projected run-off anomalies (Figs. S8e, f).

1 Deser, C., Tomas, R., Alexander, M., and Lawrence, D.: The seasonal atmospheric response to projected Arctic Sea ice loss in the late twenty-first century, J. Climate, 23, 333-351, doi: 10.1175/2009JCLI3053.1, 2010.

2 Nghiem, S. V., D. K. Hall, T. L. Mote, M. Tedesco, M. R. Albert, K. Keegan, C. A. Shuman, N. E. DiGirolamo, and G. Neumann (2012), The extreme melt across the Greenland ice sheet in 2012, Geophys. Res. Lett., 39, L20502, doi:10.1029/2012GL053611.

7 Near surface temperature: RCM vs GCM

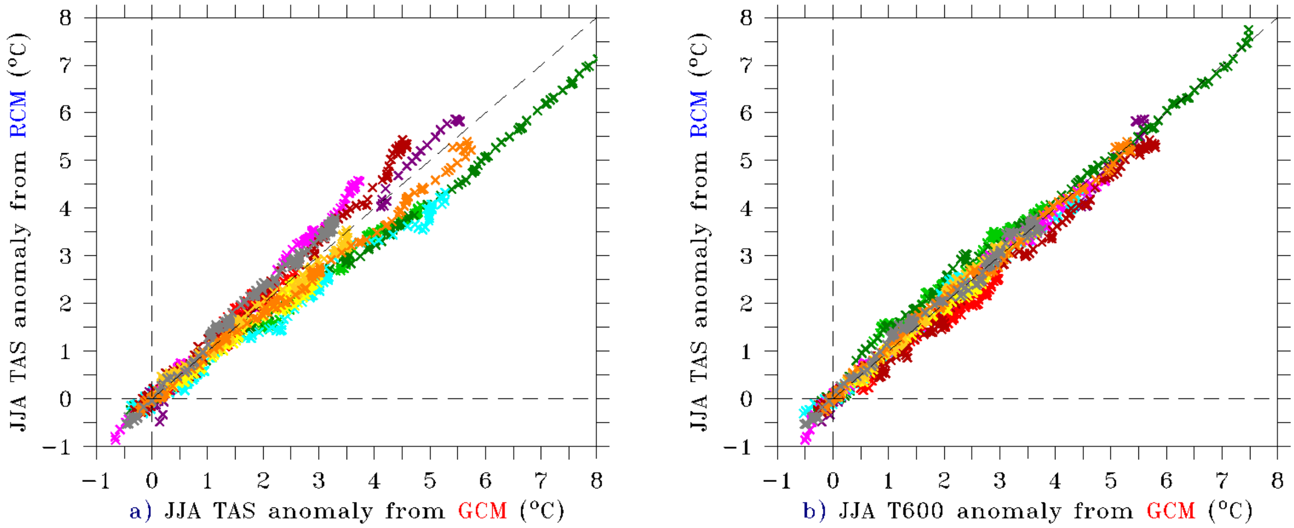

***Fig. S9**: Left) JJA TAS anomaly from RCM vs the one from GCM with respect to 1980-1999. In lack of an ice sheet mask in the GCMs, the pixels located in the area described above and at an altitude higher than 1000 meters a.s.l are used for computing the JJA TAS over GrIS. The topography (OROG) of each model is used for selecting the pixels higher than 1000 m a.s.l. Right) The same as left but for T600 computed over the area (70°W-20°W and 60°N-85°N). Finally, a 10-yr running mean has been applied for smoothing the curves.*

Depending on the forcing GCM, the GCM underestimates or overestimates the JJA TAS changes simulated by the forced RCM over GrIS while JJA T600 anomaly from GCM and JJA TAS anomaly from RCM compare well. This shows that the variability of the RCM based TAS does not depend on the GCM based TAS and that using TAS anomaly coming from GCM for evaluating changes over GrIS could be questionable with respect to RCMs using a physically based surface scheme well adapted and validated over GrIS. This highlights the interest of using RCMs for studying near-surface changes.

8 Estimation of GrIS SMB using GCM outputs

	Corr.	RMSE (GT/yr)
MARv2 $_{\text{CanESM2}}$ vs CanESM2 (RCP45)	0.84	89
MARv2 $_{\text{CanESM2}}$ vs CanESM2 (RCP85)	0.97	104
MARv2 $_{\text{MIROC5}}$ vs MIROC5 (RCP45)	0.84	84
MARv2 $_{\text{MIROC5}}$ vs MIROC5 (RCP85)	0.96	92
MARv2 $_{\text{NorESM1-M}}$ vs NorESM1-M (RCP45)	0.86	69
MARv2 $_{\text{NorESM1-M}}$ vs NorESM1-M (RCP60)	0.85	84
MARv2 $_{\text{NorESM1-M}}$ vs NorESM1-M (RCP85)	0.94	77

Table S3*: Statistics (coefficient of correlation and RMSE in GT/yr) comparing time series plotted in Fig. 8c and Fig. 8d i.e. the GrIS SMB simulated by MARv2 vs the GrIS SMB derived with Eq. 1 from the forcing outputs over 2000-2100 (without having applied a 10-yr running mean).*

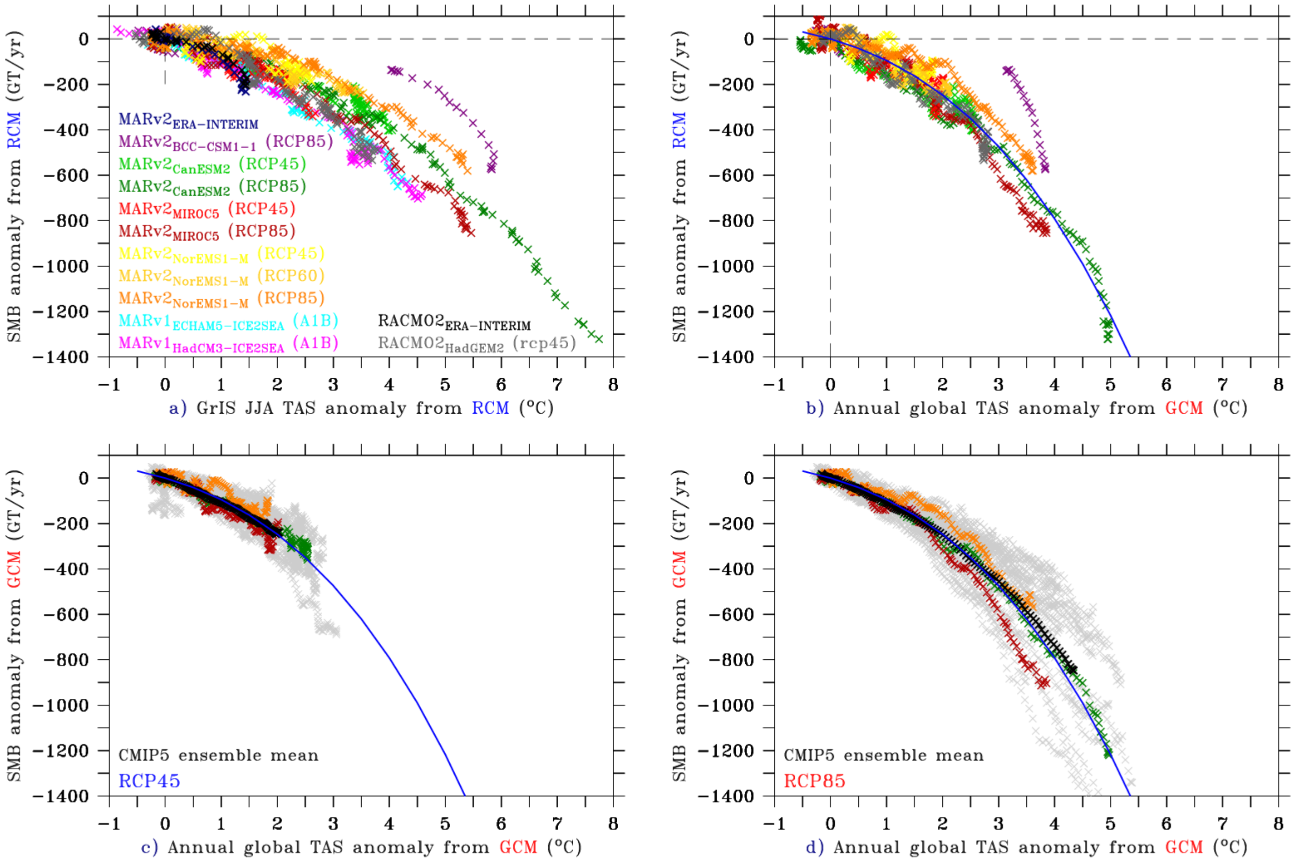

***Fig. S10**: a) GrIS SMB anomaly from RCM vs JJA TAS anomaly from RCM with respect to 1980-1999. b) GrIS SMB anomaly from RCM vs global annual TAS from GCM. c) GrIS SMB anomaly estimated from GCM outputs using Eq. 1 vs global annual TAS from GCM for the RCP45 scenario. d) Same as c) but for the RCP85 scenario. Finally, in blue, there is an approximation of the GrIS SMB anomalies (in GT/yr) following:*

$$\Delta\, SMB = -2.8(\Delta\, TAS)^3 - 20.4(\Delta\, TAS)^2 - 71.5(\Delta\, TAS)$$

where $\Delta\, TAS$ *(in °C) is the global annual TAS anomaly from GCM with respect to 1980-1999. A 10-yr running mean has been applied for smoothing the curves of all time series.*